Computational and Structural Biotechnology Journal 18 (2020) 3555–3566

COMPUTATIONAL AND STRUCTURAL BIOTECHNOLOGY JOURNAL

journal homepage: www.elsevier.com/locate/csbj

Deciphering rice metabolic flux reprograming under salinity stress via *in silico* metabolic modeling

Kwanjeera Wanichthanarak [a,b], Chuthamas Boonchai [c,d], Thammaporn Kojonna [c], Supachitra Chadchawan [c], Wichian Sangwongchai [e], Maysaya Thitisaksakul [e,*]

[a] Siriraj Metabolomics and Phenomics Center, Faculty of Medicine Siriraj Hospital, Mahidol University, Bangkok 10700, Thailand
[b] Metabolomics and Systems Biology, Department of Biochemistry, Faculty of Medicine Siriraj Hospital, Mahidol University, Bangkok 10700, Thailand
[c] Center of Excellence in Environment and Plant Physiology, Department of Botany, Faculty of Science, Chulalongkorn University, Bangkok 10330, Thailand
[d] Future Innovation and Research in Science and Technology, Chulalongkorn University, Bangkok 10330, Thailand
[e] Department of Biochemistry, Faculty of Science, Khon Kaen University, Khon Kaen 40002, Thailand

ARTICLE INFO

Article history:
Received 26 August 2020
Received in revised form 12 November 2020
Accepted 13 November 2020
Available online 20 November 2020

Keywords:
Rice (*Oryza sativa* L.)
Salinity stress
Systems biology
Metabolic flux analysis
Metabolic modeling
Transcriptomics
Metabolomics
Multi-omics analysis

ABSTRACT

Rice is one of the most economically important commodities globally. However, rice plants are salt susceptible species in which high salinity can significantly constrain its productivity. Several physiological parameters in adaptation to salt stress have been observed, though changes in metabolic aspects remain to be elucidated. In this study, rice metabolic activities of salt-stressed flag leaf were systematically characterized. Transcriptomics and metabolomics data were combined to identify disturbed pathways, altered metabolites and metabolic hotspots within the rice metabolic network under salt stress condition. Besides, the feasible flux solutions in different context-specific metabolic networks were estimated and compared. Our findings highlighted metabolic reprogramming in primary metabolic pathways, cellular respiration, antioxidant biosynthetic pathways, and phytohormone biosynthetic pathways. Photosynthesis and hexose utilization were among the major disturbed pathways in the stressed flag leaf. Notably, the increased flux distribution of the photorespiratory pathway could contribute to cellular redox control. Predicted flux statuses in several pathways were consistent with the results from transcriptomics, end-point metabolomics, and physiological studies. Our study illustrated that the contextualized genome-scale model together with multi-omics analysis is a powerful approach to unravel the metabolic responses of rice to salinity stress.

1. Introduction

Rice (*Oryza sativa* L.) is a staple food for global population and is one of the most economically important crops with the world gross production of 780 million tons in 2018 [1]. However, it is the most salt susceptible cultivar among the cereal crops for which moderately saline soil can reduce the yield by 50% [2,3]. As such, increasing rice productivity is even more challenging when the degree of soil salinization increases. As a consequence of elevated global temperature, drought, and poor agricultural practices [4], it was expected that saline soils could cover 50% of all arable land globally by the next 30 years [5]. Different rice genotypes possess different salt-tolerant degrees, ranging from highly susceptible to salt-tolerant cultivars [6]. The plasticity of rice productivity can be impacted by both severity of salt stress and different stages of crop growth [7]. The NaCl concentration above 40 mM is generally con-

Abbreviations: ADH, Arogenate dehydrogenase; ASA, Ascorbate; CGS, Cystathionine γ-synthase; CINV, Cytosolic invertase; GC-TOF-MS, Gas chromatography time-of-flight mass spectrometry; GEM, Genome-scale metabolic model; GSH, Glutathione; GSSG, Glutathione disulfide; GAPDH, Glyceraldehyde-3-phosphate dehydrogenase; GMD, Golm Metabolome Database; IAA, Indole-3-acetic acid; IPA, Indolepyruvate; iMAT, Integrative Metabolic Analysis Tool; Ci, Intercellular CO2 concentration; MDH, Malate dehydrogenase; MAPK, Mitogen-activated protein kinase; Pn, Net photosynthesis rate; PLS-DA, Partial-Least Squares Discriminant Analysis; PFK, Phosphofructokinase; 3-PGA, 3-Phosphoglycerate; GLYK, 3-Phosphoglycerate kinase; PGK, Phosphoglycerate kinase; gs, Stomatal conductance; SOD, Superoxide dismutase; E, Transpiration rate; TAT, Tyrosine aminotransferase.

* Corresponding author.
E-mail addresses: kwanjeera.wan@mahidol.ac.th (K. Wanichthanarak), mayath@kku.ac.th (M. Thitisaksakul).

https://doi.org/10.1016/j.csbj.2020.11.023

sidered harmful to rice [2], but salinity imposed at the reproductive stage can lead to more considerable yield loss [7,8].

Generally, salinity stress affects plants in two distinct stages. It first impedes plant cells from absorbing water due to the 'osmotic effect' of salt ions and later disrupts normal cellular activities due to the 'ion toxicity effect' of salt [3,9,10], ultimately altering plant metabolism. Several features of the plant salt stress responses are moderated by different but overlapping signal transduction pathways, resulting in metabolic reprograming, and physiological and morphological adaptations [11,12]. Reduction in photosynthetic capacity is evident in plants exposed to saline conditions [13]. Immediate mobilization of leaf starch is observed in salt-sensitive varieties of *Arabidopsis* and tomato under high salt conditions [12,14], however, over-accumulation of root starch has shown to possibly contribute to better salt tolerance in rice [15]. Several plants adapt to osmotic stress by over-accumulating small metabolites such as sugars, sugar alcohols, proline, and betaines to lower cellular osmotic potential and maintain water-absorbing capacity, while preserving macromolecules from damage [9,16]. Interestingly, some sugars can also act as signal molecules regulating and modulating plant metabolic activities on many levels [17].

Exposing leaf and shoot to high salt causes oxidative stress, leading to an increase in H_2O_2, glutathione disulfide (GSSG), lipid peroxidation, and eventually electrolyte leakage, accompanied by surged activity of superoxide dismutase (SOD), glutathione reductase, and peroxidase [18,19]. The accumulation of several secondary metabolites such as flavonoids, polyphenols, anthocyanin, or polyamines in plants are also observed [20]. In addition, several plant hormones including abscisic acid, auxin, cytokinins, brassinosteroids, jasmonate, gibberellin, and ethylene play an important role in mediating alleviation of salt stress in plants [21]. Most studies have emphasized on the effects of salinity stress on physiology, gene expression, enzyme activity and the end-point metabolic products of pathways, meanwhile changes in metabolic reaction rates (i.e., fluxes) are not as widely investigated [17]. The analysis of flux states displays the result of multilayered regulation of metabolite synthesis, degradation, and conversion through the intertwined metabolic pathways [17], reflecting the metabolic status of the cells.

Genome-scale metabolic models (GEMs) are valuable systems biology platforms to investigate metabolic scenarios underlying a particular cellular condition. A GEM of an organism comprises all metabolic reactions, which are represented in a mathematical framework for flux simulations and phenotype predictions [22]. GEMs have been fruitfully utilized for both biological discoveries [23] and metabolic engineering [24]. Furthermore, extracting context-specific models (e.g. cell line-, tissue- or disease-specific metabolic models) is an advanced use of GEMs by integrating with omics and experimental data. It has been stated that the extracted models can predict metabolic states more accurately than generic GEMs [25]. To date, GEMs are available for more than 6000 different organisms [26]. There are three GEMs reconstructed for rice, each of which is equipped with different features e.g. number of genes, reactions, compartments and metabolites coverage [27]. The rice GEMs have been employed in deciphering chlorophyll biosynthesis [28], the study to increase rice yield [29] and the studies of rice responses to environmental changes [27,30–32], but not in salinity stress. The successful implementation of the rice GEMs in previous studies lends support to the application of the approach to investigate how fluxes in the rice plants are reprogrammed under salinity stress. The outcomes will be a step towards unraveling and fine-tuning rice adaptability to saline soil.

In the present study, a systems biology approach was utilized to characterize metabolic states of rice flag leaf in response to high salinity. The analysis steps of this study are summarized in Fig. 1. Transcriptomics data were integrated to the rice GEM for outlining context-specific models: salt stress model and non-stress model. The extracted models were investigated for metabolic patterns under these conditions. Integrative analysis of transcriptomics, metabolomics, and physiological response data in combination with the flux states shed light on how rice responses to salt stress in the context of metabolism.

2. Materials and methods

2.1. Plant materials

Seeds of rice (*Oryza sativa* L. var. 'Nipponbare') were germinated for seven days. Then rice seedlings were transferred to grow in pots containing five kilograms of soil by using randomized complete block design (RCBD) with three replications per condition. The rice plants were grown in the greenhouse of Botany Department, Faculty of Science, Chulalongkorn University, and Biology Department, Faculty of Science, Khon Kaen University until reaching reproductive stage. At booting stage, for the salt stress condition, water was removed and 150 mM NaCl solution was added into the pots, whereas no NaCl solution was added for the control condition. After cultivated for nine more days, flag leaves of both control and salt stress conditions were collected for RNA and metabolite extraction.

2.2. Transcriptomics analysis

In total, there were 12 samples of RNA-seq data; six salinity stress samples and six control samples. Complete sample preparation and data analysis are explained in Boonchai et al. (2018) [33]. Briefly, total RNA was extracted from rice flag leaf samples of both control and salt stress conditions by using Invitrogen's Concert™ Plant RNA Reagent. Then DNaseI (NEB) was added in order to eliminate contaminated genomic DNA. cDNA libraries were prepared by The KAPA Stranded RNA-Seq Library Preparation Kit for Illumina® (Kapa biosystem, USA). Fragments with size of ~300 bp were selected and connected to adaptors. After that, all fragments were enriched by PCR for 12 cycles and all cDNA libraries were sequenced by Illumina Next-Generation sequencing (Illumina, USA). All short-sequence reads without adaptor were grouped by following the method from Missirian et al. [34]. The sequence reads were mapped to rice reference genome prior to differential gene expression analysis using the R package DESeq [35].

2.3. Metabolomics analysis

For metabolite profiling, 30 mg of rice flag leaf were extracted according to previously described protocol [36]. The standards including 20 μL of 0.2 mg/mL Ribitol (Sigma Aldrich, Singapore) and 20 μL of 0.2 mg/mL Norleucine (Sigma Aldrich, Singapore) were added to the extracts. Similar to transcriptomics data, there were six salinity stress samples and six control samples. The samples were shipped to the NIH West Coast Metabolomics Center, University of California, Davis for derivatization and quantification of primary metabolites by gas chromatography time-of-flight mass spectrometry (GC-TOF-MS) using previously described protocol [37]. Mass spectra were acquired and further processed by the BinBase database [38,39]. Raw data, given as peak heights for the quantification ion, was normalized by the sum of all peak heights for all annotated metabolites. Prior to statistical analysis, the normalized data were natural logarithm transformed using the Metabox toolbox [40].

Multivariate analysis using a partial least squares discriminant analysis (PLS-DA) approach was performed with the R package ropls [41]. Significantly altered metabolites of rice under salinity

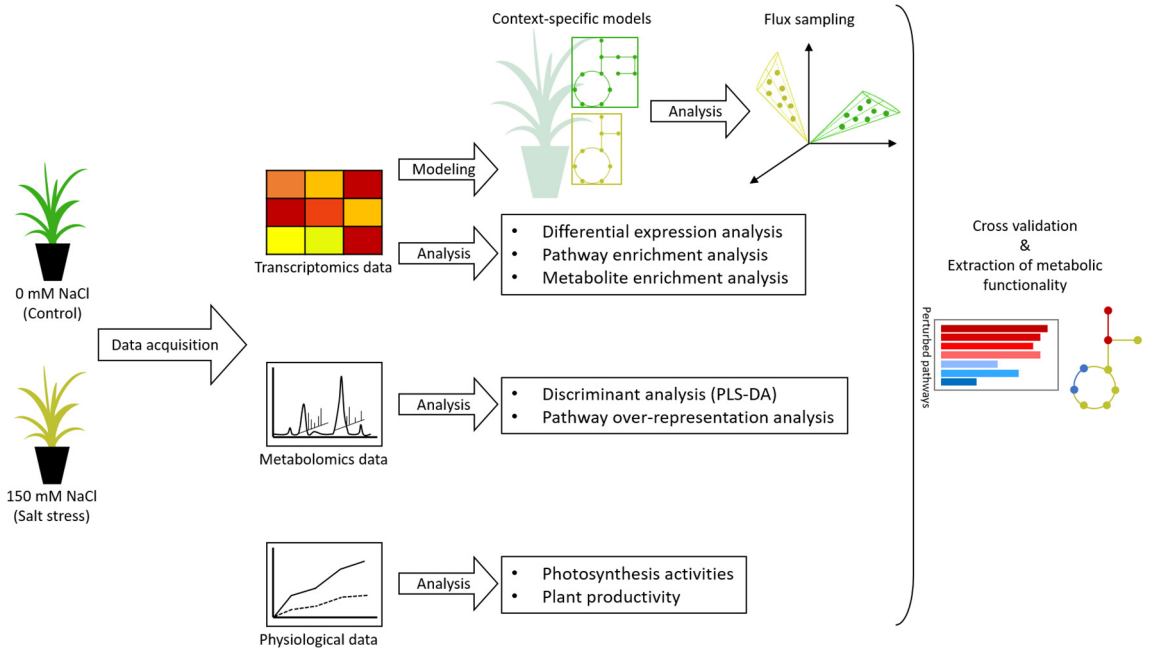

Fig. 1. Analysis workflow. Rice at booting stage was cultivated in two conditions: no salt treatment (control) and 150 mM NaCl treatment (salt stress). Flag leaves of both conditions were collected for transcript and metabolite profiling. The model contextualization was performed based on transcriptomics data to construct context-specific models before metabolic flux analysis. Omics data and *in silico* metabolic modeling were combined to characterized metabolic activities of rice under salt stress. PLS-DA, partial least squares-discriminant analysis.

stress were identified by considering variable importance in projection (VIP) values [42]. Only metabolites with VIP >1.0 were considered as important discriminants between two conditions. The log2-fold change (log2FC) of each metabolite was estimated to represent increase or decrease levels of the metabolite under salt stress relative to control condition.

Structurally unknown metabolites were further predicted by using the Golm Metabolome Database (GMD) [43]. The GMD database contains mass spectral and retention index (RI) information of metabolites quantified by GC–MS platforms. The database estimates quality of mass spectral matching by using mass intensity information and provides as distance scores (1-dotprod distance by default). The scores range from 0 to 1; 0 represents perfect match and 1 denotes complete mismatch.

2.4. Pathway and metabolite enrichment analysis

For transcriptomics data, the p-values and the log2-fold changes from the differential gene expression analysis were used as the inputs for pathway enrichment analysis and metabolite enrichment analysis. The pathway enrichment analysis was performed to identify perturbed pathways in salinity stress compared to control condition. The metabolite enrichment analysis, (i.e., the reporter metabolite analysis) was conducted to pinpoint metabolites within the rice GEM that surrounded by significant transcriptional changes [44]. The analyses were performed using the Reporter Features algorithm [45] implemented on the R package piano [46]. This method classifies the directionality of gene expression changes into up- or down- regulation or both to aid interpretation of the results.

For metabolomics data, pathway over-representation analysis was calculated with Fisher's exact test as implemented on the R package piano. Chemical category over-representation analysis was performed using the Metabox toolbox. Only important metabolites with VIP >1.0 from PLS-DA were used in these analyses.

Biochemical pathway information from the KEGG database [47] was used for the pathway analysis. Pathways and metabolites with p-value <0.01 were considered as significantly altered in salt stress condition.

2.5. Extraction of context-specific models

The salt stress-specific model and non-stress model of rice leaves were extracted from the rice GEM *i*OS2164 [30] coupled with the transcriptomics data. The *i*OS2164 model is fully compartmentalized, composed of 2165 genes, 2444 reactions and 1999 metabolites, and delineates light-driven photophosphorylation reactions for five light spectra (red, blue, green white and dark). In this study, only white light reactions, which are the mixture of red, blue and green reactions, and the straw biomass reaction were included in the calculation. We used the Integrative Metabolic Analysis Tool (iMAT) algorithm [48,49] to extract the context-specific models. The method integrates gene or protein expression data to the GEMs. It aims to maximize the number of flux-carrying reactions associated with highly expressed genes (i.e. minimizing the number of non-zero flux reactions associated with lowly expressed genes), so that a steady-state metabolic flux distribution satisfies stoichiometric and thermodynamic constraints of the model. The transcriptomics data were regularized logarithm (rlog) transformed using the R package DESeq2 [50]. Average expression values were used by the iMAT algorithm. Highly expressed genes were determined by their expression level above $\mu + 0.5\sigma$ and lowly expressed genes were ones with the expression level below $\mu - 0.5\sigma$ [49], where μ denotes average expression level across all genes of each condition and σ is the associated standard deviation (SD). The analysis with iMAT algorithm was conducted as implemented in the COBRA toolbox [51] in MATLAB.

2.6. Random sampling and differential flux analysis

To simulate photorespiration of rice leaves, the constraints of flux solution space were implemented by limiting the photon uptake at 100 mmol g^{-1} DCW h^{-1} [30] and excluding red light, blue

light, green light and coleoptile biomass reactions. For each context-specific GEM, reaction fluxes were uniformly sampled by using the Artificial Centering Hit-and-Run (ACHR) Monte Carlo sampling [52,53] algorithm implemented in the COBRA toolbox. 5000 flux samples were obtained for each reaction. Then, for each condition, all flux samples of reactions were normalized by using the following equation (Eq. (1)). Briefly, each flux value of a sample point was divided by the sum of all fluxes of that sample point [54].

$$normalizedflux_{ij} = \frac{flux_{ij}}{\sum_{i=1}^{n} abs(flux_{ij})} \quad (1)$$

n denotes number of reactions, i designates i^{th} reaction and j is j^{th} sample point.

After that, the differences in flux samples between salinity stress and control condition were computed by randomly choosing two normalized flux vectors, one from flux samples of each condition, and calculating both the differences and relative flux ratios. This process was repeated to create 10,000 flux difference samples for each reaction. The reaction Z scores indicate flux differences between two conditions and was calculated as illustrated in Eq. (2) [55].

$$Z_i = \frac{abs(\mu_i)}{\sigma_i/\sqrt{n}} \quad (2)$$

μ denotes sample mean, σ is standard deviation and i designates i^{th} reaction.

P-values were derived from the absolute Z scores based on cumulative distribution function of normal distribution. The obtained p-values were adjusted for multiple testing with Benjamini and Hochberg at a false discovery rate (FDR) of 0.05.

2.7. Flux-sum analysis

The flux-sum for a metabolite represents its turnover rate, which is calculated from the summation of fluxes of reactions around the metabolite (Eq. (3)) [56].

$$f_i = 0.5 \sum_i abs(S_{xi} v_i) \quad (3)$$

S_{xi} denotes stoichiometric coefficient of metabolite x of reaction i, and v_i designates flux of reaction i.

The log2-ratios of flux-sum values between salt stress and control condition were qualitatively compared to the directional changes of metabolite abundance.

2.8. Physiological response of rice flag leaf and plant productivity under salinity stress

Rice seeds were germinated and planted in soil as indicated above. At booting stage, 150 mM NaCl was added to reach soil EC of 7–9 $dS.m^{-1}$, while water was added to the control plants (non-stress). Then, photosynthesis parameters, net photosynthesis rate and stomatal conductance of the flag leaves were determined after 1, 3, 6 and 9 days after salt-stresses treatment by using LI-6400 XT portable photosynthesis system (LI-COR, Lincoln, NE). For plant productivity, rice grains were harvested for the assessment of the percentage of unfilled grain and total grain yield. The experiment was performed with six replicates per treatment. The differences were deemed significant at p-value <0.05 by student's *t*-test.

3. Results and discussion

3.1. Pathways and metabolites from transcriptomics alterations

Pathway enrichment analysis was carried out to identify disturbed pathways in salt stress condition compared to control condition based on transcriptomics data. We considered pathways that were enriched by either up-regulated or down-regulated genes in response to 150 mM NaCl treatment. Several biosynthesis pathways in rice flag leaf were altered. These include phenylalanine, tyrosine, glutathione (GSH), and isoquinone metabolisms, and oxidative phosphorylation that were enriched by up-regulated genes, whereas antenna protein biosynthesis and Mitogen-activated protein kinase (MAPK) signaling pathway were affected by transcriptional downregulation (Fig. 2 and Supplementary Table S1). Likewise, genes associated with phenylalanine, tyrosine and tryptophan metabolism, oxidative phosphorylation, indole-3-acetic acid (IAA) biosynthesis, starch metabolism, GSH metabolism, brassinosteroids biosynthesis, terpenoid biosynthesis via MEP pathway, mitochondrial fatty acid biosynthesis, and mitochondrial transport were up-regulated, while photosynthetic water-water cycle, thiamine metabolism, and cellulose metabolism were enriched by down-regulated genes (Supplementary Table S2). Besides pathway-level information, we identified the metabolic hotspots (i.e., reporter metabolites that indicate perturbed regions at metabolite level) within the rice metabolic network. Metabolites associated by up-regulated genes were methionine, ubiquinone, ubiquinol, tryptamine, 2-oxoglutarate, amino acids (such as leucine, tyrosine and alanine), serotonin, raffinose and myo-inositol, while metabolites that were affected by down-regulated genes included galactose 1-phosphate, galactose, adenylosuccinic acid, 1-aminocyclopropane-1-carboxylic acid (ACC), and acetate (Fig. 3 and Supplementary Table S3).

Previous transcriptomics studies of salt-tolerant rice (cv.Pokkali) response to salinity stress show the enrichment of Gene Ontology (GO) terms including oxidation reduction, terpenoid biosynthesis, glutathione-metabolic processes, activation of kinase activity, and response to auxin stimulus [57]. The other study reports late response genes (1–3 days post 200 mM NaCl treatment), which include up-regulated genes in primary plant metabolism and stress protective genes, and down-regulated set of genes involved in photosynthesis and protein synthesis [58]. Consistently, our gene expression analysis revealed up-regulation of genes in oxidative phosphorylation, and aromatic amino acid, GSH and isoquinone metabolism, while the genes in photosynthetic antenna protein and MAPK signaling pathways were majorly down-regulated (Fig. 2 and Supplementary Table S1).

3.2. Metabolome analysis of rice leaf responses to salinity stress

Metabolomics analysis reported 444 metabolites in total, of which 143 were structurally annotated. We observed clear separation between salt-induced and control samples indicating there were metabolic changes in rice under the stress (Supplementary Fig. S1). In addition, biological variations between each salt-treated flag leaf were greater than the control samples (Supplementary Fig. S1). Of the 444 reported metabolites, 157 were discriminative metabolites (VIP > 1.0) between the salt stress and control conditions (Supplementary Table S4). Among these, 61 metabolites had known annotation, and we predicted 91 structurally unknown metabolites using the GMD database.

The top metabolites capturing metabolic variations across conditions included sugars (e.g., allose, glucose, raffinose, maltotriose, 2,7-anhydro-sedoheptulose, melibiose), sugar alcohols (e.g., xylitol, galactinol), organic acids (e.g., malic acid, α-ketoglutaric acid,

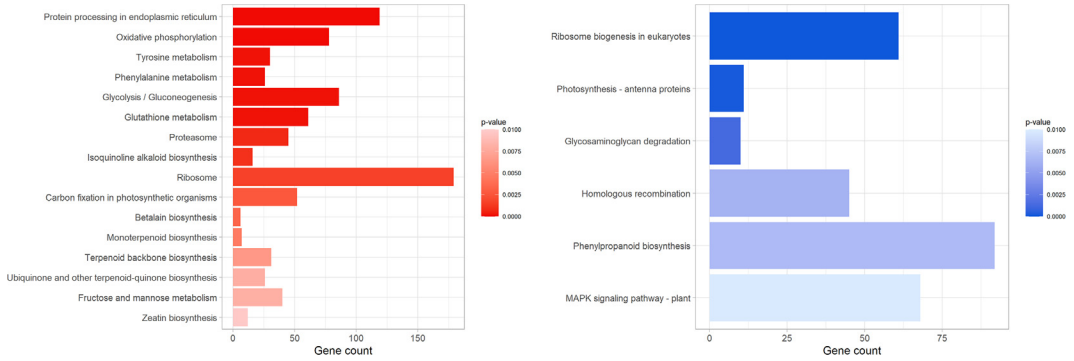

Fig. 2. Disturbed pathway determined from transcriptomics analysis. Left figure illustrates the pathways significantly enriched by distinctly up (red)- regulated genes, whereas right figure is the pathways enriched by down (blue)-regulated genes. Significantly enriched pathways are the pathways with p-value <0.01. (For interpretation of the references to color in this figure legend, the reader is referred to the web version of this article.)

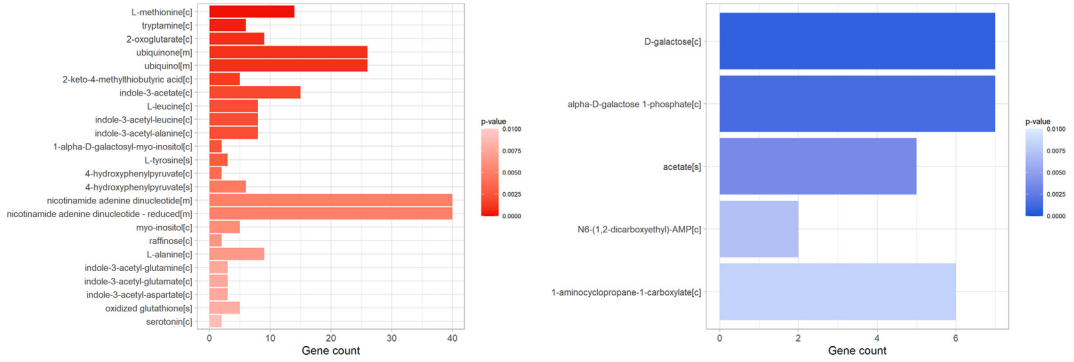

Fig. 3. Perturbed metabolites determined from transcriptomics analysis. Left figure illustrates the metabolites significantly surrounded by distinctly up (red)- regulated genes, whereas right figure is the metabolites surrounded by down (blue)-regulated genes. Significantly enriched metabolites are the metabolites with p-value <0.01. (For interpretation of the references to color in this figure legend, the reader is referred to the web version of this article.)

2-phosphoglyceric acid, malonic acid, oxalic acid, 6-phosphogluconic acid, 4-aminobutanoic acid), antioxidative compounds (e.g., ascorbic acid, 3,4-dihydroxybenzoic acid), nucleobase (e.g., adenine), alcohols (e.g., 1,2,4-butanetriol), amino acids and their derivatives (e.g., serine, tyramine, phenylalanine, threonine, leucine, cycloleucine, isoleucine, pyroglutamic acid, glycine, sarcosine, α-aminoadipic acid), amine (e.g., ethanolamine) and amino sugar (e.g., galactosamine) (Supplementary Table S4). Chemical categories based on Medical Subject Headings (MeSH – chemicals and drugs) [59] that were over-represented by the discriminative metabolites were listed in Supplementary Table S5.

Pathways overrepresented by the discriminant metabolites were identified (Table 1). Interestingly, the altered pathways based on transcriptional changes (Fig. 2 and Supplementary Table S1) were also picked out from metabolomics profiles (Table 1). These pathways were aromatic amino acid, secondary metabolite, and GSH metabolism. Changes in such cellular metabolism could be a result of gene expression alterations. The oxidative phosphorylation pathway was enriched by up-regulated genes based on the transcriptomics analysis alone (Fig. 2 and Supplementary Table S1). However, its upstream pathway, TCA cycle, was identified based on the additional metabolomics information (Table 1).

Table 1
Pathways overrepresented by discriminative metabolites.[1]

Pathway name	No. of metabolites in pathway	Metabolite count	pval	qval
Aminoacyl-tRNA biosynthesis	52	14	2.96E−15	3.14E−13
ABC transporters	138	14	3.70E−09	1.96E−07
Alanine, aspartate and glutamate metabolism	28	7	7.84E−08	2.77E−06
Phenylalanine, tyrosine and tryptophan biosynthesis	35	7	4.12E−07	1.09E−05
Cyanoamino acid metabolism	45	7	2.49E−06	5.28E−05
Glyoxylate and dicarboxylate metabolism	62	7	2.24E−05	0.000395765
Biosynthesis of various secondary metabolites – part 2	73	7	6.57E−05	0.000995643
Arginine biosynthesis	23	4	0.000273671	0.003223232
Valine, leucine and isoleucine biosynthesis	23	4	0.000273671	0.003223232
Glucosinolate biosynthesis	77	6	0.000711221	0.007538941
Glutathione metabolism	38	4	0.00194549	0.018747453
Citrate cycle (TCA cycle)	20	3	0.002678215	0.023657569
Taurine and hypotaurine metabolism	22	3	0.003545398	0.028908632
Glycine, serine and threonine metabolism	50	4	0.005346365	0.040479623

[1] The table is sorted by pval and shows the pathways that are significantly overrepresented by discriminative metabolites (pval < 0.01). qval, q-value or the-p-value adjusted with Benjamini and Hochberg at FDR = 0.05.

Other pathways including aminoacyl-tRNA biosynthesis, ABC transporters, several amino acid metabolism, cyanoamino acid metabolism, glyoxylate and dicarboxylate metabolism, and glucosinolate biosynthesis were associated with discriminant metabolites (Table 1).

3.3. Generation of salt stress-specific models

We used the rice GEM *i*OS2164 as a template for the extraction of salt stress- and non-stress-specific models based on the transcriptomics evidence. The total of 1939 metabolic genes in the *i*OS2164 model were mapped to the gene expression profiles for the context-specific model extraction using the iMAT algorithm. In particular, there are three main families of algorithms for context-specific model extraction: Gene Inactivity Moderated by Metabolism and Expression (GIMME)-like, iMAT-like and Model Building Algorithm (MBA)-like families, as explained by [60]. The iMAT algorithm from the iMAT-like family was used in this study, as it does not require a metabolic objective in contrast to the GIMME-like family. This method is appropriate in our context where no clear objective function is pre-defined for rice experiencing environmental changes. The MBA-like family was not considered in this study because it requires a priori defined set of high confidence reactions, being active in a certain context.

The iMAT algorithm requires a user-specified gene expression threshold to determine which genes are expressed. In this study, we explored three different thresholds: $\mu \pm 0.5\sigma$, $\mu \pm \sigma$ and $\mu \pm 2\sigma$ (Supplementary Fig. S2). Less number of genes were used by the algorithm to extract context-specific models when the threshold was increased (Supplementary Fig. 2A). Approximately, 30%, 11% and 2% of 1939 metabolic genes were highly expressed based on the observed thresholds, respectively. We further examined the biomass objective values of the extracted models from each threshold. The biomass reaction fluxes of control- and salt-specific models (from $\mu \pm 0.5\sigma$ threshold) were 90.7% and 92.1% of optimal growth rate of *i*OS2164 leaf cell model, as predicted by flux balance analysis [53] Supplementary Figure S2 (Supplementary Fig. 2B). While the biomass objective values of other extracted models were less than 90%. Therefore, we chose the gene expression threshold of half a SD above and below the mean for highly expressed and lowly expressed genes, respectively.

Approximately 1200 reactions (half of the reactions in the *i*OS2164 model) were in the active state. Of these, 1157 reactions were active in both conditions, while 44 and 45 reactions were only active in control and salt stress models, respectively (Supplementary Fig. S3). Flux distributions for each model were computed by the uniform random sampling for subsequent analyses. This approach computes a large set of possible flux solutions and does not require an objective function [61].

3.4. Flux statuses in rice metabolic subsystems

Metabolic fluxes for each context-specific model were computed, and flux differences between two conditions were estimated. The reactions with adjusted p-values <0.01 were considered as statistically different between salt stress and control conditions. A set of significant reactions were subsequently discussed according to their subsystems (Figs. 4–6).

3.4.1. Metabolic fluxes of primary metabolic pathways

Modifications in fluxes among different primary metabolic pathways in response to salinity stress were investigated (Fig. 4). Despite the up-regulation of 52 out of 77 genes involved in photosynthesis carbon fixation (Supplementary Table S1), small flux changes through the reactions catalyzed by Calvin-Benson cycle enzymes and photophosphorylation were observed (Fig. 4A). However, the flux state of chloroplastic glyceraldehyde-3-phosphate dehydrogenase (GAPDH) reaction was very much reduced (log2FC = −4.19) in salt stress condition (Fig. 4A). GAPDH in higher plants exists as the supramolecular complex with CP12 small protein, which contributes to the overall regulation of photosynthetic metabolism [62]. The significant reduction in the flux of GAPDH reaction may suggest reduced photosynthetic activities in the salt-stressed flag leaf, as previously demonstrated by the transcriptome study of rice seedling exposed to high salinity (150 and 200 mM NaCl) [58,63]. Although the reduced activities in Calvin-Benson cycle was not directly observed via transcriptomics and metabolmics analysis, the downregulated antenna protein biosynthetic genes also supported the overall reduction of photosynthesis under salinity stress (Fig. 2 and Supplementary Table S1). Reduction of photosynthetic rate was previously observed in mature rice leaf under salinity stress [13,64–66]. This could be a result of (i) direct inhibition of enzyme by accumulated ions (ii) reduced stomatal conductance or (iii) the feedback inhibition of accumulated sugars, which act as osmoticum in the tissue [64–67].

Similar to photosynthesis, overall fluxes in photorespiration pathways were not critically changed (Fig. 4B). However, the flux through 3-phosphoglycerate kinase (GLYK; log2FC = 3.22) reaction was greatly magnified in the salt-treated condition. GLYK catalyzes the last step in the photorespiration pathway [68] and the increase in flux suggests higher photorespiration activity of plant tissues, as evident in higher plants [69]. Photosynthesis and photorespiration are obligatory interwinding metabolic processes [68]. Inefficient photosynthesis due to the decrease in stomatal conductance under stress condition could be accompanied by high photorespiratory rate as the enzyme Ribulose biphosphate carboxylase/oxygenase (RuBisCo) is available for O_2 substitution in the first step of photosynthetic CO_2 fixation [68,70]. Flux prediction also pointed out the salt-stressed rice flag leaf favor in reversing 2-phosphoglycerate kinase reaction to yield glycerate, which could be a substrate for either hydroxypyruvate or 3-phosphoglycerate (3-PGA) synthesis in glycolate-glyoxylate metabolism [68,71]. These findings were supported by the metabolomics evidence, which showed that glyoxylate metabolim was overrepresented by the discriminant metabolites (Table 1).

Overall fluxes through starch biosynthesis were not affected except for a distinct decline in fluxes through the reactions of amylo 1–6-glucosidase, which is a debranching enzyme [72], and α-amylase in the salinity-stressed leaf (Fig. 4C). Similarly, the flux in sucrose biosynthesis was slightly affected by salinity except for the reduction of fluxes through cytosolic invertase (CINV; log2FC = −0.83) and fructokinase (FRK; log2FC = −0.14) reactions (Fig. 4C). These reductions suggest reduced cellular hexose availability and utilization for cell growth and development [72–74]. This could, however, be a result of reduced sink activity such as a delayed parnicle emergence or an abortion of developing rice seed [2,75].

For primary cell wall metabolism, fluxes through fructose, inositol-phosphate and amino sugars metabolism were slightly changed under salinity, while the significant modification in flux was observed in galactose metabolism (Fig. 4D). The fluxes through the reactions catalyzed by galactinol-raffinose galactosyltransferease (log2FC = 1.11) and stachyose galactohydrolase were greatly enhanced in salt stress condition (Fig. 4D). These enzymes play an important role in stachyose biosynthesis, which is observed even in senescent and partially yellowed leaves [76]. In addition, the flux via raffinose synthase was substantially reduced in the salt-treated leaf (Fig. 4D), supporting the favor in galactosyltransfer activity towards synthesizing stachyose rather than raffinose. This result suggests the shift from starch metabolism to other storage carbohydrate metabolism in the salt-stressed flag leaf.

Metabolic changes were distinctly observed in amino acid metabolism (Fig. 4E). Fluxes markedly increase in cysteine and

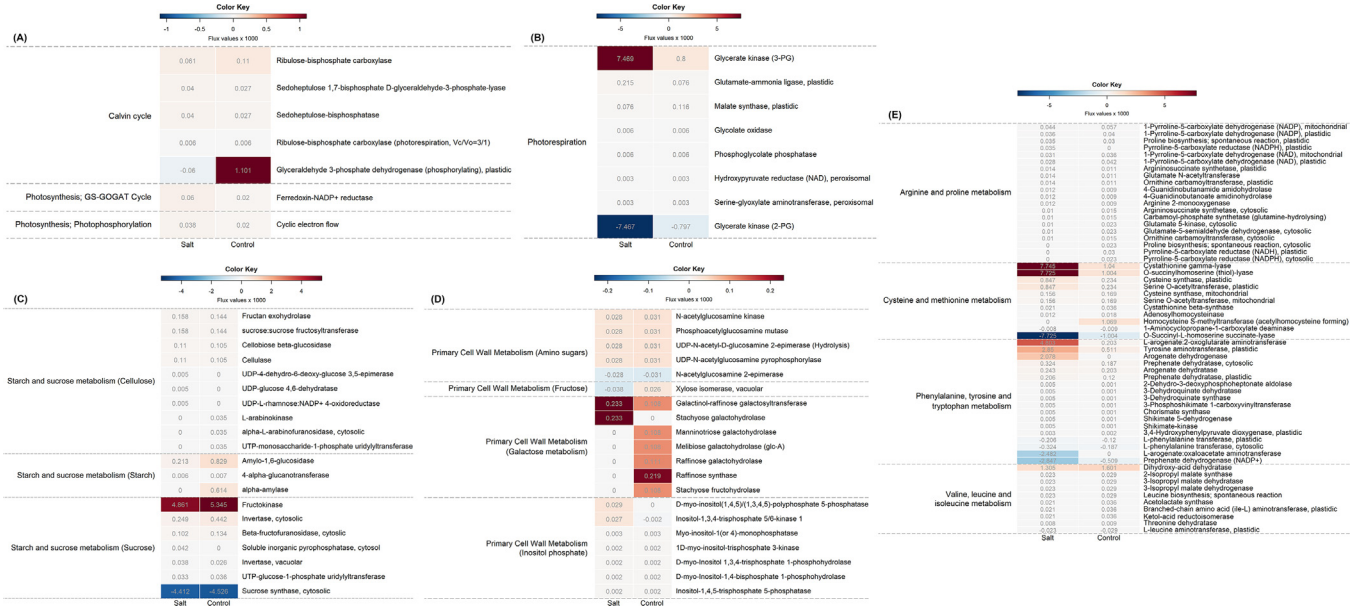

Fig. 4. Flux states of primary metabolic pathways across conditions. (A) Photosynthesis, (B) Photorespiration, (C) Starch and sucrose metabolism, (D) Primary cell wall metabolism, and (E) Amino acid metabolism. Reactions are in row and conditions are in column. For each heatmap, the color intensity corresponds to the average magnitude of each reaction flux sample. Red and blue colors represent forward and reverse direction of each reaction. The left hand color key indicates the subsystem of individual reaction. (For interpretation of the references to color in this figure legend, the reader is referred to the web version of this article.)

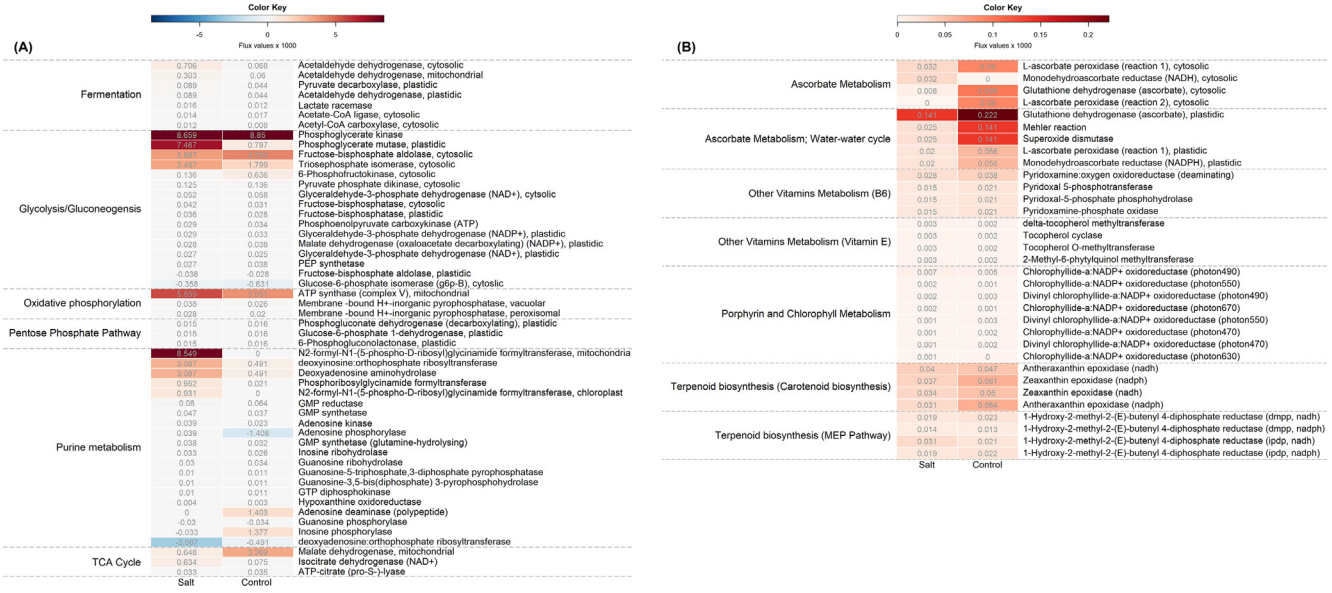

Fig. 5. Flux states of cellular respiration and antioxidant biosynthetic pathways. (A) Cellular respiration (B) Antioxidant metabolism. Reactions are in row and conditions are in column. For each heatmap, the color intensity corresponds to the average magnitude of each reaction flux sample. Red and blue colors represent forward and reverse direction of each reaction. The left hand color key indicates the subsystem of individual reaction. (For interpretation of the references to color in this figure legend, the reader is referred to the web version of this article.)

methionine metabolism, but the flux towards taurine synthesis was strongly affected under salinity stress condition. *O*-succinyl-L-homoserine succinate-lyase reaction favored *O*-succinyl-L-homoserine and L-cysteine synthesis, meanwhile the flux through reactions that were catalyzed by its orthologs, cystathionine γ-synthase (CGS) and *O*-succinylhomoserine (thiol)-lyase, preferred L-cystathionine and succinate synthesis (Fig. 4E) [77]. Whether these three enzymes work in a complimentary or antagonistic manner in this stress condition required further investigation. The fluxes of tyrosine amino-transferease (TAT; log2FC = 2.48), arogenate dehydrogenase (ADH), and L-arogenate:oxaloacetate aminotransferase (aka prephenate aminotransferease) reactions were enhanced under salt stress compared to control condition (Fig. 4E), suggesting an increase in aromatic amino acid metabolism of salinity-induced rice [78–80]. Flux predictions of taurine biosynthesis and aromatic amino acid metabolism from the context-specific models matched with the findings from metabolomics profiles, as both were also overrepresented by discriminative metabolites (Table 1).

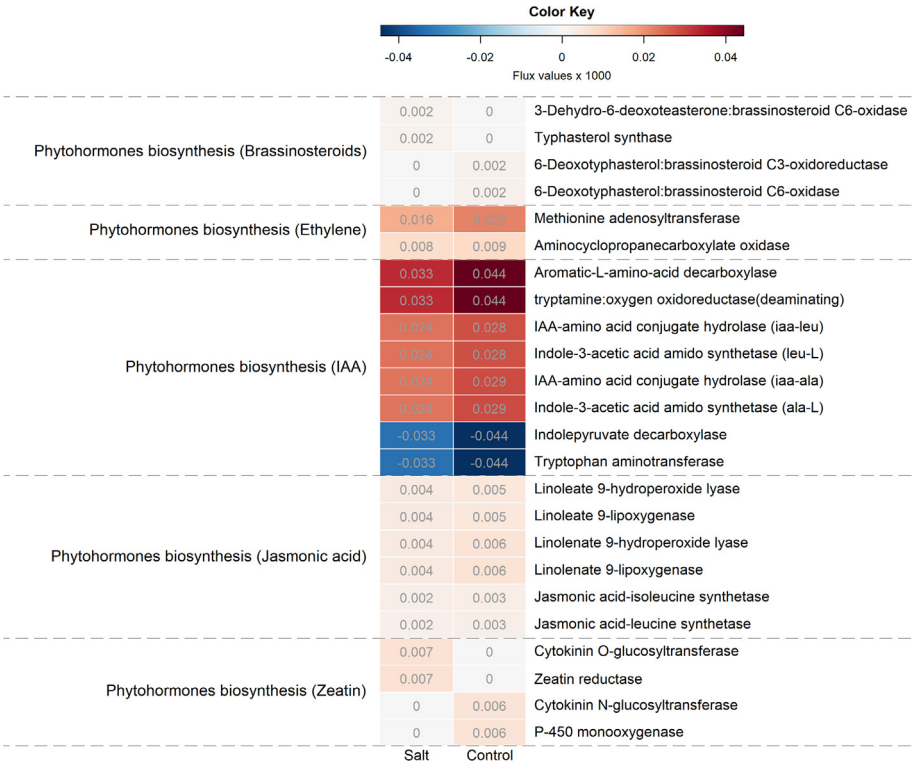

Fig. 6. Flux states of phytohormone biosynthesis. Reactions are in row and conditions are in column. The color intensity corresponds to the average magnitude of each reaction flux sample. Red and blue colors represent forward and reverse direction of each reaction. The left hand color key indicates the subsystem of individual reaction. (For interpretation of the references to color in this figure legend, the reader is referred to the web version of this article.)

3.4.2. Metabolic fluxes of cellular respiration and antioxidant biosynthetic pathways

Metabolic functions of cellular respiration and antioxidant biosynthetic pathways were investigated to observe potential oxidative stress responses and its alleviation under salinity stress condition (Fig. 5). There was no obvious flux change among reactions in pentose phosphate pathway and fermentation (Fig. 5A). However, for glycolytic pathway, we noticed a huge flux increase in the reactions of phosphoglycerate mutase (log2FC = 3.23) and triosephosphate isomerase (log2FC = 1.0), and a flux decrease in the key enzyme phosphofructokinase (PFK; log2FC = −2.23) and phosphoglycerate kinase (PGK; log2FC = −0.03) under salt stress condition (Fig. 5A). Taken together, the decreased flux through rate-limiting step catalyzed by PFK suggests the suppression in glycolytic activity under salinity, which is in agreement with previous transcriptomics and proteomics studies [63,81]. In addition, reduction of glycolysis resulted in less production of substrate for TCA cycle activity, which was in line with the flux reduction of malate dehydrogenase (MDH; log2FC = −2.38) reaction (Fig. 5A), as well as over-representation of discriminative metabolites in TCA cycle (Table 1). The reduced glycolysis and TCA activities were in line with the observed high flux magnitude through cysteine and methionine metabolism, and aromatic amino acid metabolism (Fig. 4E and Fig. 5A). The use of glycolytic and TCA intermediates for amino acid synthesis was previously described as one of the adaptive mechanisms in the salt-treated barley [63]. In addition, aromatic amino acid, such as phenylalanine is a precursor for both biosynthesis of salicylic acid (a regulator of salt-tolerant signaling pathway [81]), and phenylpropanoid (an important player in antioxidative system under salt stress [82]) metabolism.

For oxidative phosphorylation, we observed significant increase in flux via mitochondrial ATP synthase (log2FC = 0.57), which was coroborating with the transcriptional upregulation of genes in this pathway (Fig. 2). Furthermore, the flux of *de novo* purine biosynthesis was much larger in salt stress condition than control condition (Fig. 5A), suggesting a substantial amount of precursor synthesized for energy compounds and electron carriers or nucleotide cofactors such as ATP and NAD, respectively [82]. Nonetheless, the flux prediction of antioxidant metabolism indicated minimal oxidative stress or ROS scavenging activity. Flux predictions showed strong reduction in fluxes of carotenoid biosynthesis under salt stress condition (Fig. 5B), and the down-regulation of antenna protein biosynthesis genes was highlighted in transcriptomics analysis (Fig. 2 and Supplementary Table S1). Our analysis implicates that less excessive light energy would have been captured by the stressed rice. In parallel, we also observed remarkable flux reduction in ascorbate (ASA) metabolism and water-water cycle (Fig. 5B). This was evident in the reduction in fluxes through the Mehler and SOD reactions, as well as the reduced flux through cytosolic and plastidic ascorbate peroxidase (APX; log2FC = −1.49), glutathione dehydrogenase (aka dehydroascorbate reductase; DHAR; log2FC = −0.65) and plastidic monodehydroascorbate reductase (MDHAR; log2FC = −1.49), implicating less production of ASA (Fig. 5B) [83]. Altogether, this reduced flux distribution in water-water cycle and ASA-GSH cycle suggested minimal photoreduction of O_2 and thus the overall oxidative stress activities in salt-treated rice leaf. This chloroplastic redox homeostasis could be attributed to the markedly increased activity of GLYK of the glycolate pathway (Fig. 4B). Chloroplast GLYK is activated by oxidative modification [84] and its product, 3-PGA, could be exchanged for the cytosolic inorganic phosphate as an important mechanism for reductant export from the chloroplast [85,86]. Therefore, our results suggest the role of flux reprogramming in photorespiration contributing to cellular redox homeostasis under this salt stress condition.

3.4.3. Metabolic fluxes of phytohormone biosynthetic pathways

Phytohormones play critical role in regulating cellular responses to modulate plant growth and development under salinity stress [21]. Therefore, the flux statuses of different plant hormone biosynthetic pathways were examined (Fig. 6). Auxin is one of the key hormones regulating plant growth and development [21,87]. Under control condition, the reversed flux in tryptophan-dependent IAA synthesis through tryptophan amino transferase (TAA1) and indolepyruvate (IPA) decarboxylase reactions [87,88]. However, the IPA decarboxylase was only isolated in microorganisms and whether it is functional in higher plants remains inconclusive [87]. Under the salt stress condition, the reversed fluxes were less preferential implying slightly increased flux towards tryptophan-dependent IAA synthesis. However, notable decrease in fluxes through enzymatic reactions that maintain auxin homeostasis by conjugating IAA to amino acid (e.g. IAA–amido synthetase) [89] was observed in salinity stress. Likewise, previous studies demonstrate that salt stress can reduce auxin synthesis and redistibute auxin maxima formation, resulting in reduced growth and development [21,90]. Interestingly, tryptophan biosynthesis, a precursor for IAA synthesis, was overrepresented by discriminative metabolites under salinity condition (Table 1). Besides, we found methionine adenosyltransferase reaction (log2FC = −0.44) in methionine-dependent ethylene synthesis had slight flux reduction [91]. Ethylene triggers downstream signaling pathways and gene expression, leading to salt stress tolerance mechanism [21]; however, the reduced flux activity in ethylene synthesis in this study suggests the inability of the flag leaf to cope with high salt, at least, via this regulator.

3.4.4. Integrative analysis of metabolic fluxes and metabolomics data

Flux analysis of the extracted models revealed metabolic reprograming in several important pathways under salt stress (Fig. 7A). We observed the directional changes of flux-sum values and com-

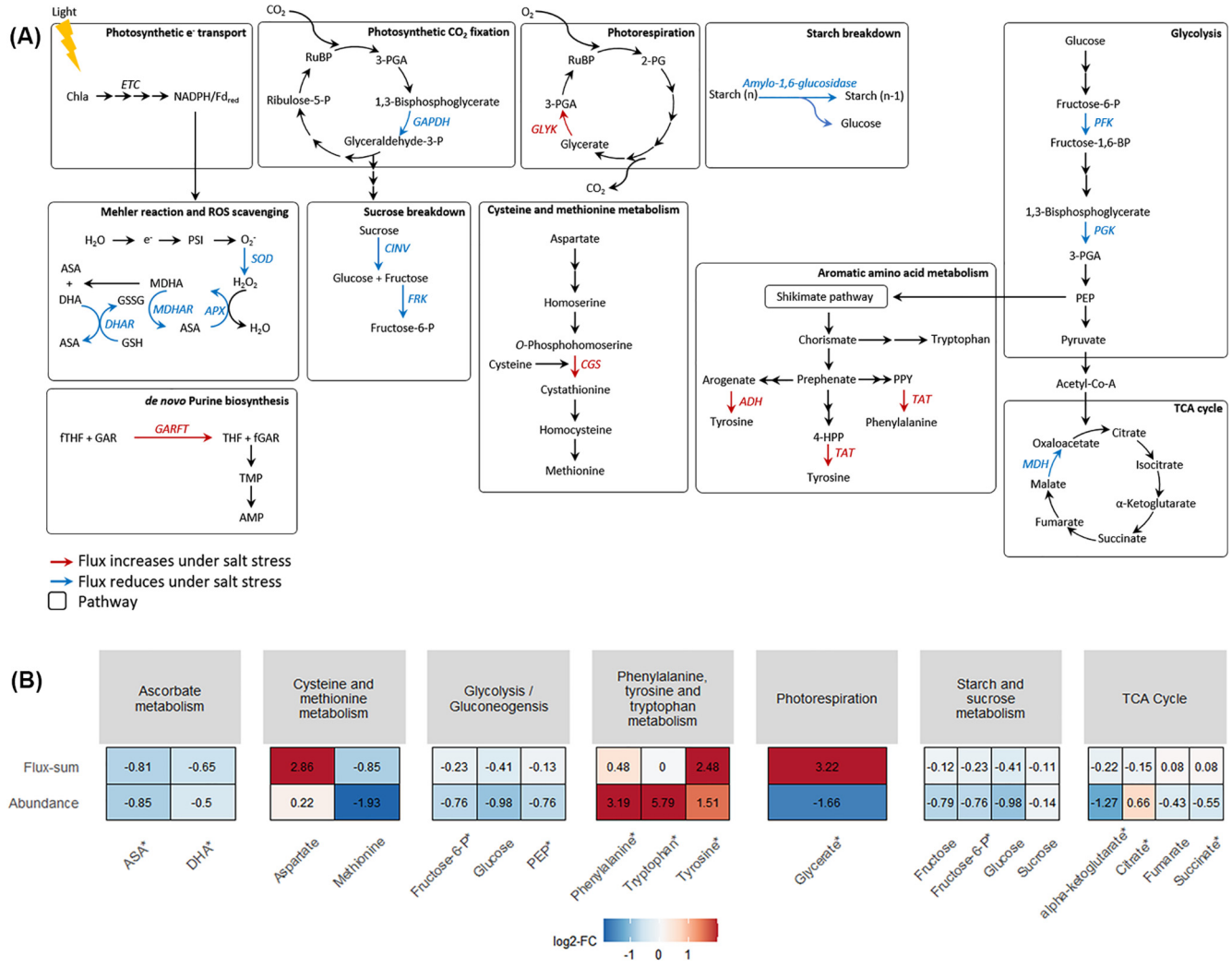

Fig. 7. (A) Flux activities in primary metabolic pathways of rice flag leaf under salinity stress. The enzyme names and arrows in red and blue indicate increases and decreases in fluxes through the reactions, respectively. (B) Comparison of the ratios of flux-sum values and metabolite abundance. Red and blue indicate increases and decreases in flux-sums and metabolite levels of rice under salt stress compared to control condition. Discriminative metabolites are marked with asterisk (*). ADH – Arogenate dehydrogenase; APX – Ascorbate peroxidase; ASA – Ascorbate; CGS – Cystathionine γ-synthase; Chla – Chlorophyll *a*; CINV – Cytosolic invertase; DHA – Dehydroascorbate; DHAR – Dehydroascorbate reductase; ETC – Electron transport chain; Fdred – Reduced ferredoxin; fGAR – 5′-Phosphoribosylformylglycinamide; FRK – Fructokinase; fTHF – 10-Formyltetrahydrofolate; GAPDH – Glyceraldehyde 3-phosphate dehydrogenase; GAR – 5-Phosphoribosylglycinamide; GARFT – Phosphoribosylglycinamide formyltransferase; GLYK – 3-Phosphoglycerate kinase; GSH – Glutathione; GSSG – Glutathione disulfide; 4-HPP – 4-Hydroxyphenylpyruvate; MDH – Malate dehydrogenase; MDHA – Monodehydroascorbate; MDHAR – Monodehydroascorbate reductase; PEP – Phosphoenolpyruvate; PFK – Phosphofructokinase; 2-PG – 2-Phosphoglycolate; 3-PGA – 3-Phosphoglycerate; PGK – Phosphoglycerate kinase; PPY – Phenylpyruvate; PSI – Photosystem I; RuBP – Ribulose 1,5-bisphosphate; SOD – Superoxide dismutase; TAT – Tyr aminotransferase; THF – Tetrahydrofolate; TMP – Thymidine monophosphate. (For interpretation of the references to color in this figure legend, the reader is referred to the web version of this article.)

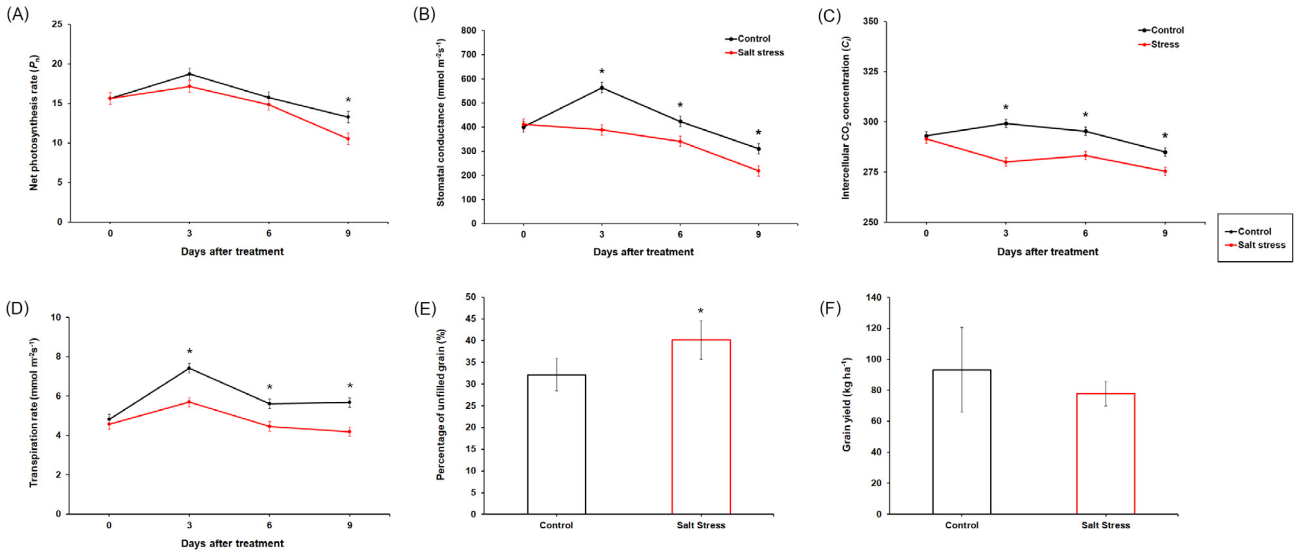

Fig. 8. Physiological responses (A-D) of rice flag leaf and plant productivity (E-F) under salinity stress. (A) Net photosynthesis rate (B) Stomatal conductance (C) Intercellular CO_2 concentration (D) Transpiration rate (E) Percentage of unfilled grain (F) Grain yield. The asterisk (*) indicates statistical difference (p-value <0.05) between control and salt stress conditions by student's *t*-test (n = 6).

pared them to the ratios of metabolite abundance among these pathways (Fig. 7B). Reduction in both flux-sum values and metabolite abundance was observed in ascorbate metabolism, glycolysis/gluconeogenesis, starch and sucrose metabolism and α-ketoglutarate of TCA cycle. The reaction fluxes in those pathways were also decreased. Meanwhile, increase in both flux-sum values and metabolite levels was noticed in aromatic amino acid metabolism (Fig. 7B) and the activities of corresponding enzymes: TAT and ADH, were increased under salt stress condition (Fig. 7A). Together, these results suggest that enhanced biosynthesis of aromatic amino acid, such as phenylalanine and tyrosine could be at the expense of glycolytic and TCA intermediates [63]. Low abundance of sugars (fructose, fructose-6-P, glucose and sucrose) in starch and sucrose metabolism (Fig. 7B) was possibly due to the reduced activity of the upstream pathway, photosynthesis in particular (Fig. 7A). Strong increase in flux-sum values (log2FC = 3.22) and decrease in metabolite level (log2FC = −1.66) of glycerate in photorespiration (Fig. 7B) was presumably as a result of the high activity of GLYK reaction (Fig. 7A). Integrative exploration of metabolome and flux predictions enables further identification of metabolic relations between reaction fluxes and altered metabolites of rice under salinity stress. These GME-predicted alterations in metabolic pathway lay a groundwork for further functional elucidation through enzymatic activity analysis, flux-feeding analysis, or through functional characterization of the genetic expression and its regulators under salinity stress condition.

3.5. Physiological response of rice flag leaf and yield response under salinity stress

Photosynthetic activities of rice flag leaf were observed at 0, 3, 6 and 9 days after salinity application (Fig. 8A–D). Net photosynthesis rate (*Pn*) of both control and salinity stressed leaves increased at day 3, but decreased after 6 and 9 days of salinity stress (Fig. 8A). The *Pn* of salt-treated flag leaf was significantly lower than that of the control after 9 days of salt exposure (Fig. 8A). The trend of photosynthetic process observed from this experiment confirmed the flux predictions of this pathway by *in silico* modeling. That included the reduction in the flux of GAPDH reaction (Fig. 4A) and the lower amount of total fluxes in photosynthetic pathway of salt stress condition (the flux ratio = 0.14; Supplementary Table S6). Reduction in *Pn* was accompanied by reduced stomatal conductance (g_s) (Fig. 8B). Salt-treated leaf exhibited less g_s than the control throughout the salt treatment period, which was also reflected in its lower intercellular CO_2 concentration (C_i) and transpiration rate (E) at all time points (Fig. 8B-8D). The percentage of unfilled grain were enhanced by salinity stress (Fig. 8E), indicating the reduced sink activity of endosperm starch synthesis. Therefore, the predicted flux reduction in starch and sucrose breakdown in the 'source' flag leaf (Fig. 4C) was well-supported by the declined 'sink' activity. Accordingly, total grain yield appeared to be impeded by salinity although the differences were masked by variation among individuals in the control group (Fig. 8F). Collectively, the flux distribution predicted by the *in silico* metabolic modeling was corroborated by the photosynthetic and yield responses of rice to salinity stress.

4. Conclusion

In the current study, the control- and salt-specific model extraction based on transcriptomics data was performed, prior to comparative analysis of metabolic fluxes between both conditions. Under salinity stress, the model predicted reduction in photosynthesis and hexose utilization, whereas increase in photorespiration was anticipated. We cross validated the predicted fluxes with trends of metabolite levels from metabolomics and physiological data to assess the robustness of model prediction. Our study addressed the key benefits of GEM, which is a powerful tool for deciphering metabolic reprograming of rice and other plants in responses to environmental changes. We highlighted that imposing gene expression constraints can better elucidate metabolisms of rice under a particular condition. Moreover, the *in silico* metabolic modeling allows researchers to readily target specific metabolic pathways or enzymes for further functional analysis, avoiding laborious stable isotope flux-feeding experiment.

Funding

This research was funded by The Thailand Research Fund and Office of the Higher Education Commission (grant number MRG6180292), Thailand.

CRediT authorship contribution statement

Kwanjeera Wanichthanarak: Conceptualization, Methodology, Software, Formal analysis, Writing - original draft, Visualization. **Chuthamas Boonchai:** Formal analysis, Investigation. **Thammaporn Kojonna:** Formal analysis, Investigation. **Supachitra Chadchawan:** Formal analysis, Resources, Supervision. **Wichian Sangwongchai:** Investigation. **Maysaya Thitisaksakul:** Conceptualization, Methodology, Resources, Writing - original draft, Visualization, Project administration, Funding acquisition.

Declaration of Competing Interest

The authors declare that they have no known competing financial interests or personal relationships that could have appeared to influence the work reported in this paper.

Acknowledgments

Work in M.T. lab was supported by the Salt-tolerant Rice Research Group, Khon Kaen University. Our gratitude is extended to Prof. Oliver Fiehn, Dr. Jutarop Phetcharaburanin, and Dr. Sakda Khoomrung for their advices on metabolite extraction and analysis. K.W. thanks Assoc. Prof. Intawat Nookaew and Dr. Natapol Pornputtapong for valuable advices in flux and statistical analysis. We also thank Dr. Narumol Jariyasopit for insightful comments.

Appendix A. Supplementary data

Supplementary data to this article can be found online at https://doi.org/10.1016/j.csbj.2020.11.023.

References

[1] FAOSTAT. FAOSTAT Crop Statistics, 2020; Available from: http://www.fao.org/faostat/en/#data/QC.
[2] Abdullah Z, Khan MA, Flowers TJ. Causes of sterility in seed set of rice under salinity stress. J Agron Crop Sci 2001;187(1):25–32.
[3] Munns R, Tester M. Mechanisms of salinity tolerance. Annu Rev Plant Biol 2008;59:651–81.
[4] Thitisaksakul M et al. Effects of environmental factors on cereal starch biosynthesis and composition. J Cereal Sci 2012;56(1):67–80.
[5] Smith AM et al. Environmental stress. New York: Garland Press; 2009.
[6] Kanawapee N et al. Genetic diversity analysis of rice cultivars (Oryza sativa L.) differing in salinity tolerance based on RAPD and SSR markers. Electron J Biotechnol 2011;14(6):2.
[7] Thitisaksakul M et al. Effects of timing and severity of salinity stress on rice (Oryza sativa L.) yield, grain composition, and starch functionality. J Agric Food Chem 2015;63(8):2296–304.
[8] Munns R. Genes and salt tolerance: bringing them together. New Phytol 2005;167(3):645–63.
[9] Hasegawa PM et al. Plant cellular and molecular responses to high salinity. Annu Rev Plant Biol 2000;51(1):463–99.
[10] Liang W et al. Plant salt-tolerance mechanism: a review. Biochem Biophys Res Commun 2018;495(1):286–91.
[11] Xiong L, Schumaker KS, Zhu J-K. Cell signaling during cold, drought, and salt stress. Plant Cell 2002;14(suppl 1):S165–83.
[12] Kempa S et al. A central role of abscisic acid in stress-regulated carbohydrate metabolism. PLoS ONE 2008;3(12).
[13] Chaves MM, Flexas J, Pinheiro C. Photosynthesis under drought and salt stress: regulation mechanisms from whole plant to cell. Ann Bot 2009;103(4):551–60.
[14] Khelil A, Menu T, Ricard B. Adaptive response to salt involving carbohydrate metabolism in leaves of a salt-sensitive tomato cultivar. Plant Physiol Biochem 2007;45(8):551–9.
[15] Thitisaksakul M et al. Overexpression of GSK3-like Kinase 5 (OsGSK5) in rice (Oryza sativa) enhances salinity tolerance in part via preferential carbon allocation to root starch. Funct Plant Biol 2017;44(7):705–19.
[16] Hýskova V, Ryslava H. Hyperosmotic versus hypoosmotic stress in plants. Biochem Anal Biochem 2018;7:1–4.
[17] Smith AM, Stitt M. Coordination of carbon supply and plant growth. Plant Cell Environ 2007;30(9):1126–49.
[18] Dionisio-Sese ML, Tobita S. Antioxidant responses of rice seedlings to salinity stress. Plant Sci 1998;135(1):1–9.
[19] Fadzilla NAM, Finch RP, Burdon RH. Salinity, oxidative stress and antioxidant responses in shoot cultures of rice. J Exp Bot 1997;48(2):325–31.
[20] Akula R, Ravishankar GA. Influence of abiotic stress signals on secondary metabolites in plants. Plant Signaling Behav 2011;6(11):1720–31.
[21] Ryu H, Cho Y-G. Plant hormones in salt stress tolerance. J Plant Biol 2015;58(3):147–55.
[22] Nilsson A, Nielsen J. Genome scale metabolic modeling of cancer. Metab Eng 2017;43(Pt B):103–12.
[23] Reed JL et al. Systems approach to refining genome annotation. Proc Natl Acad Sci U S A 2006;103(46):17480–4.
[24] Park JH et al. Metabolic engineering of Escherichia coli for the production of L-valine based on transcriptome analysis and in silico gene knockout simulation. Proc Natl Acad Sci U S A 2007;104(19):7797–802.
[25] Opdam S et al. A systematic evaluation of methods for tailoring genome-scale metabolic models. Cell Syst 2017;4(3):318–329.e6.
[26] Gu C et al. Current status and applications of genome-scale metabolic models. Genome Biol 2019;20(1):121.
[27] Lakshmanan M et al. Modeling rice metabolism: from elucidating environmental effects on cellular phenotype to guiding crop improvement. Front Plant Sci 2016;7:1795.
[28] Chatterjee A, Kundu S. Revisiting the chlorophyll biosynthesis pathway using genome scale metabolic model of Oryza sativa japonica. Sci Rep 2015;5:14975.
[29] Shaw R, Kundu S. Flux balance analysis of genome-scale metabolic model of rice (Oryza sativa): Aiming to increase biomass. J Biosci 2015;40(4):819–28.
[30] Lakshmanan M et al. Unraveling the light-specific metabolic and regulatory signatures of rice through combined in silico modeling and multiomics analysis. Plant Physiol 2015;169(4):3002–20.
[31] Poolman MG et al. Responses to light intensity in a genome-scale model of rice metabolism. Plant Physiol 2013;162(2):1060–72.
[32] Lakshmanan M et al. Elucidating rice cell metabolism under flooding and drought stresses using flux-based modeling and analysis. Plant Physiol 2013;162(4):2140–50.
[33] Boonchai C et al. Rice overexpressing OsNUC1-S reveals differential gene expression leading to yield loss reduction after salt stress at the booting stage. Int J Mol Sci 2018;19(12).
[34] Missirian V et al. Pope: pipeline of parentally-biased expression. International symposium on bioinformatics research and applications. Springer; 2012.
[35] Anders S, Huber W. Differential expression analysis for sequence count data. Genome Biol 2010;11(10):R106.
[36] Weckwerth W, Wenzel K, Fiehn O. Process for the integrated extraction, identification and quantification of metabolites, proteins and RNA to reveal their co-regulation in biochemical networks. Proteomics 2004;4(1):78–83.
[37] Fiehn O et al. Quality control for plant metabolomics: reporting MSI-compliant studies. Plant J 2008;53(4):691–704.
[38] Fiehn O, Wohlgemuth G, Scholz M. Setup and annotation of metabolomic experiments by integrating biological and mass spectrometric metadata. 2005. Berlin, Heidelberg: Springer Berlin Heidelberg.
[39] Scholz M, Fiehn O. SetupX–a public study design database for metabolomic projects. Pac Symp Biocomput 2007:169–80.
[40] Wanichthanarak K et al. Metabox: A toolbox for metabolomic data analysis, interpretation and integrative exploration. PLoS ONE 2017;12(1):e0171046.
[41] Thevenot EA et al. Analysis of the human adult urinary metabolome variations with age, body mass index, and gender by implementing a comprehensive workflow for univariate and OPLS statistical analyses. J Proteome Res 2015;14(8):3322–35.
[42] Wheelock AM, Wheelock CE. Trials and tribulations of 'omics data analysis: assessing quality of SIMCA-based multivariate models using examples from pulmonary medicine. Mol BioSyst 2013;9(11):2589–96.
[43] Hummel J et al. Mass spectral search and analysis using the Golm metabolome database. In: The handbook of plant metabolomics. p. 321–43.
[44] Patil KR, Nielsen J. Uncovering transcriptional regulation of metabolism by using metabolic network topology. Proc Natl Acad Sci U S A 2005;102(8):2685.
[45] Oliveira AP, Patil KR, Nielsen J. Architecture of transcriptional regulatory circuits is knitted over the topology of bio-molecular interaction networks. BMC Syst Biol 2008;2(1):17.
[46] Varemo L, Nielsen J, Nookaew I. Enriching the gene set analysis of genome-wide data by incorporating directionality of gene expression and combining statistical hypotheses and methods. Nucleic Acids Res 2013;41(8):4378–91.
[47] Kanehisa M et al. Data, information, knowledge and principle: back to metabolism in KEGG. Nucleic Acids Res 2014;42(Database issue):D199–205.
[48] Shlomi T et al. Network-based prediction of human tissue-specific metabolism. Nat Biotechnol 2008;26(9):1003–10.
[49] Zur H, Ruppin E, Shlomi T. iMAT: an integrative metabolic analysis tool. Bioinformatics 2010;26(24):3140–2.
[50] Love MI, Huber W, Anders S. Moderated estimation of fold change and dispersion for RNA-seq data with DESeq2. Genome Biol 2014;15(12):550.
[51] Heirendt L et al. Creation and analysis of biochemical constraint-based models using the COBRA Toolbox vol 3.0. Nat Protoc 2019;14(3):639–702.
[52] Thiele I et al. Candidate metabolic network states in human mitochondria. Impact of diabetes, ischemia, and diet. J Biol Chem 2005;280(12):11683–95.
[53] Schellenberger J, Palsson BØ. Use of randomized sampling for analysis of metabolic networks. J Biol Chem 2009;284(9):5457–61.
[54] Nam H et al. A systems approach to predict oncometabolites via context-specific genome-scale metabolic networks. PLoS Comput Biol 2014;10(9):e1003837.

[55] Mo ML, Palsson BØ, Herrgård MJ. Connecting extracellular metabolomic measurements to intracellular flux states in yeast. BMC Syst Biol 2009;3(1):37.
[56] Chung BK, Lee DY. Flux-sum analysis: a metabolite-centric approach for understanding the metabolic network. BMC Syst Biol 2009;3:117.
[57] Shankar R, Bhattacharjee A, Jain M. Transcriptome analysis in different rice cultivars provides novel insights into desiccation and salinity stress responses. Sci Rep 2016;6(1):23719.
[58] Kumari S et al. Transcriptome map for seedling stage specific salinity stress response indicates a specific set of genes as candidate for saline tolerance in Oryza sativa L. Funct Integr Genomics 2008;9(1):109.
[59] Lipscomb CE. Medical subject headings (MeSH). Bull Med Libr Assoc 2000;88 (3):265–6.
[60] Robaina Estevez S, Nikoloski Z. Generalized framework for context-specific metabolic model extraction methods. Front Plant Sci 2014;5:491.
[61] Herrmann HA et al. Flux sampling is a powerful tool to study metabolism under changing environmental conditions. NPJ Syst Biol Appl 2019;5(1):32.
[62] Sparla F et al. Regulation of photosynthetic GAPDH dissected by mutants. Plant Physiol 2005;138(4):2210.
[63] Ueda A et al. Comparative transcriptome analyses of barley and rice under salt stress. Theor Appl Genet 2006;112(7):1286–94.
[64] Pal M et al. Photosynthetic characteristics and activity of antioxidant enzymes in salinity tolerant and sensitive rice cultivars. Indian J Plant Physiol 2004;9 (4):407–12.
[65] Moradi F, Ismail AM. Responses of photosynthesis, chlorophyll fluorescence and ROS-scavenging systems to salt stress during seedling and reproductive stages in rice. Ann Bot 2007;99(6):1161–73.
[66] Dionisio-Sese ML, Tobita S. Effects of salinity on sodium content and photosynthetic responses of rice seedlings differing in salt tolerance. J Plant Physiol 2000;157(1):54–8.
[67] Pattanagul W, Thitisaksakul M, Effect of salinity stress on growth and carbohydrate metabolism in three rice (Oryza sativa L.) cultivars differing in salinity tolerance. 2008.
[68] Bauwe H, Hagemann M, Fernie AR. Photorespiration: players, partners and origin. Trends Plant Sci 2010;15(6):330–6.
[69] Parida AK, Das AB. Salt tolerance and salinity effects on plants: a review. Ecotoxicol Environ Saf 2005;60(3):324–49.
[70] Di Martino C et al. Free amino acids and glycine betaine in leaf osmoregulation of spinach responding to increasing salt stress. New Phytol 2003;158 (3):455–63.
[71] Dellero Y et al. Photorespiratory glycolate–glyoxylate metabolism. J Exp Bot 2016;67(10):3041–52.
[72] Hii SL et al. Pullulanase: role in starch hydrolysis and potential industrial applications. Enzyme Res 2012;2012:921362.
[73] Barratt DHP et al. Normal growth of Arabidopsis requires cytosolic invertase but not sucrose synthase. Proc Natl Acad Sci U S A 2009;106 (31):13124.
[74] Stein O, Granot D. Plant fructokinases: evolutionary, developmental, and metabolic aspects in sink tissues. Front Plant Sci 2018;9:339.
[75] Wankhade SD et al. Morpho-physiological variations in response to NaCl stress during vegetative and reproductive development of rice. Acta Physiol Plant 2013;35(2):323–33.
[76] Avigad G, Dey PM. Carbohydrates metabolism: storage carbohydrates. In: Dey PM, Harborne JB, editors. Plant biochemistry. San Diego, CA: Academics Press; 1997. p. 143–204.
[77] Ravanel S et al. Cystathionine γ-synthase from Arabidopsis thaliana: purification and biochemical characterization of the recombinant enzyme overexpressed in Escherichia coli. Biochem J 1998;331(2):639–48.
[78] Prabhu PR, Hudson AO. Identification and partial characterization of an L-tyrosine aminotransferase (TAT) from Arabidopsis thaliana. Biochem Res Int 2010;2010.
[79] Rippert P, Matringe M. Molecular and biochemical characterization of an Arabidopsis thaliana arogenate dehydrogenase with two highly similar and active protein domains. Plant Mol Biol 2002;48(4):361–8.
[80] Maeda H, Yoo H, Dudareva N. Prephenate aminotransferase directs plant phenylalanine biosynthesis via arogenate. Nat Chem Biol 2011;7(1):19–21.
[81] Liu C-W et al. Comparative proteomic analysis of early salt stress responsive proteins in roots and leaves of rice. Proteomics 2014;14(15):1759–75.
[82] Moffatt BA, Ashihara H, Purine and pyrimidine nucleotide synthesis and metabolism. The arabidopsis book, 2002. 1: p. e0018-e0018.
[83] Strizh I. The Mehler reaction as an essential link between environmental stress and chloroplast redox signaling. In: Photosynthesis. Energy from the Sun. Springer; 2008. p. 1343–6.
[84] Bartsch O et al. An autoinhibitory domain confers redox regulation to maize glycerate kinase. Plant Physiol 2010;153(2):832.
[85] Kromer S. Respiration during photosynthesis. Annu Rev Plant Physiol Plant Mol Biol 1995;46(1):45–70.
[86] Keech O et al. The redox control of photorespiration: from biochemical and physiological aspects to biotechnological considerations. Plant Cell Environ 2017;40(4):553–69.
[87] Zhao Y. Auxin biosynthesis and its role in plant development. Annu Rev Plant Biol 2010;61(1):49–64.
[88] Tao Y et al. Rapid synthesis of auxin via a new tryptophan-dependent pathway is required for shade avoidance in plants. Cell 2008;133(1):164–76.
[89] Ding X et al. Activation of the indole-3-acetic acid-amido synthetase GH3-8 suppresses expansin expression and promotes salicylate- and jasmonate-independent basal immunity in rice. Plant Cell 2008;20(1):228–40.
[90] Kazan K. Auxin and the integration of environmental signals into plant root development. Ann Bot 2013;112(9):1655–65.
[91] Yang SF, Hoffman NE. Ethylene biosynthesis and its regulation in higher plants. Annu Rev Plant Physiol 1984;35(1):155–89.